arXiv:astro-ph/0201534v1 31 Jan 2002

THE LAS CAMPANAS DISTANT CLUSTER SURVEY - THE CORRELATION FUNCTION

Anthony H. Gonzalez[1]

Harvard-Smithsonian Center for Astrophysics, 60 Garden Street, Cambridge, MA 02138

Dennis Zaritsky

Steward Observatory, University of Arizona, 933 North Cherry Avenue, Tuscon, AZ 85721

Risa H. Wechsler[2]

Department of Physics, University of California, Santa Cruz, CA 95064

Submitted to The Astrophysical Journal

ABSTRACT

We present the first non-local ($z > 0.2$) measurement of the cluster-cluster spatial correlation length, using data from the Las Campanas Distant Cluster Survey (LCDCS). We measure the angular correlation function for velocity-dispersion limited subsamples of the catalog at estimated redshifts of $0.35 \leq z_{est} < 0.575$, and derive spatial correlation lengths for these clusters via the cosmological Limber equation. The correlation lengths that we measure for clusters in the LCDCS are consistent both with local results for the APM cluster catalog and with theoretical expectations based upon the Virgo Consortium Hubble Volume simulations and the analytic predictions. Despite samples containing over 100 clusters, our ability to discriminate between cosmological models is limited because of statistical uncertainty.

1. INTRODUCTION

The spatial correlation function of galaxy clusters provides an important cosmological test, as both the amplitude of the correlation function and its dependence upon mean intercluster separation are determined by the underlying cosmological model. In hierarchical models of structure formation, the spatial correlation length, r_0, is predicted to be an increasing function of cluster mass, with the exact dependence determined by σ_8 (or equivalently Ω_0, using the constraint on $\sigma_8 - \Omega_0$ from the local cluster mass function) and the power spectrum shape parameter, Γ. Low density and low Γ models generally predict stronger clustering for a given mass and a greater dependence of the correlation length upon cluster mass.

The three-space correlation function of clusters was first measured for subsamples of the Abell catalog by Bahcall & Soneira (1983) and Klypin & Kopylov (1983). Both groups found that the correlation function is well-described by a power law, $\xi(r) = (r/r_0)^{-\gamma}$, and obtained a correlation length $r_0 \simeq 25h^{-1}$ Mpc with $\gamma \simeq 2$. Bahcall & Soneira (1983) also observed a strong dependence of correlation strength upon cluster richness, which was later quantified by Bahcall (1988) and Bahcall & West (1992) as a roughly linear dependence of r_0 upon d_c, the mean intercluster separation. Postman, Huchra, & Geller (1992) and Peacock & West (1992) confirmed the form of the correlation function for the Abell catalog in their larger spectroscopic samples, with both studies obtaining $r_0 \simeq 20h^{-1}$ Mpc for clusters with richness class R≥1.

While these correlation lengths have strong implications for cosmological models, a key problem with interpretation of the Abell results is concern that the observed correlation lengths are positively skewed by projection effects and sample inhomogeneities (see Sutherland 1988; Dekel et al. 1989; Efstathiou et al. 1992; Peacock & West 1992). Several analyses find that $\xi(\sigma, \pi)$ is strongly anisotropic, evidence that these effects are significant (Sutherland 1988; Efstathiou et al. 1992; Peacock & West 1992). Still, the net impact of these factors is unclear.

Contrary to the concerns raised by these studies, Miller et al. (1999) use an expanded sample of Abell clusters to derive correlation lengths that are consistent with earlier analyses and robust to projection effects, and van Haarlem, Frenk, & White (1997) argue that projections are insufficient to account for the stronger correlation observed in the Abell catalog as compared to the APM catalog (Dalton et al. 1992).

Fortunately, independent constraints on the correlation function have arisen as new catalogs with automated, uniform selection criteria have become available (e.g., Dalton et al. 1992; Nichol et al. 1992; Dalton et al. 1994; Nichol, Briel, & Henry 1994; Romer et al. 1994; Croft et al. 1997; Collins et al. 2000; Moscardini et al. 2000). Some of the recent optical catalogs, such as the APM (Dalton et al. 1992), also probe to lower d_c than the Abell samples, while the X-ray samples provide greatly improved leverage for the most massive (highest d_c) clusters. While systematic variations persist between samples, the existing data are generally consistent with r_0 slowly increasing with d_c (however, see Collins et al. 2000).

To exploit the growth of observational data, there has been a corresponding theoretical effort to predict the cluster spatial correlation function as a function of mass and epoch. Driven by cosmological volume N-body simulations (e.g., Governato et al. 1999; Colberg et al. 2000; Moscardini et al. 2000) and the development of a well-tested analytic formalism (Mo & White 1996; Sheth & Tormen 1999; Sheth, Mo, & Tormen 1999), a theoretical framework has been established that enables derivation of quantitative cosmological constraints from the observational data. The mass dependence can be studied using existing data sets and is typically best matched by low-density models (see Croft et al. 1997; Borgani, Plionis, & Kolokotronis 1999b; Collins et al. 2000), although systematic uncertainties and observational scatter have precluded precision cosmological constraints. In contrast, the redshift dependence remains unconstrained because the data have not existed to test the evolutionary predictions of these models.

[1] Present Address: Department of Astronomy, University of Florida, P.O. Box 112055, Gainesville, FL 32611

[2] Present Address: Physics Department, University of Michigan, Ann Arbor, MI 48109.

In this paper we utilize the Las Campanas Distant Cluster Survey (LCDCS) to determine the spatial correlation length at $z\simeq0.45$. We first measure the angular correlation function for a series of subsamples at this epoch and then derive the corresponding r_0 values via the cosmological Limber inversion (Peebles 1980; Efstathiou et al. 1991; Hudon & Lilly 1996). The resulting r_0 values constitute the first measurement at this epoch of the dependence of the cluster correlation length upon d_c, probing mean separations similar to previous local optical catalogs. Popular structure formation models predict only a small amount of evolution from z=0.45 to the present, as illustrated in section 5. We test this prediction by comparing our results with the local observations.

2. THE LAS CAMPANAS DISTANT CLUSTER SURVEY

The recently completed Las Campanas Distant Cluster Survey, which contains 1073 candidates, is the largest published catalog of galaxy clusters at $z \gtrsim 0.3$ (Gonzalez et al. 2001). Clusters are detected in the LCDCS as regions of excess surface brightness relative to the mean sky level, a technique that permits wide-area coverage with a minimal investment of telescope time. The final statistical catalog covers an effective area of 69 square degrees within a $78^\circ \times 1.6^\circ$ strip of the southern sky ($860 \times 24.5\ h^{-1}$ Mpc at z=0.5 for Ω_0=0.3 ΛCDM). Gonzalez et al. (2001) also provide estimated redshifts, z_{est}, based upon the brightest cluster galaxy (BCG) magnitude-redshift relation that are accurate to $\sim$15% at $z_{est} = 0.5$, and demonstrate the existence of a correlation between the peak surface brightness, Σ, and velocity dispersion, σ. Together these two properties enable construction of well-defined subsamples that can be compared directly with simulations and observations of the local universe.

3. THE LCDCS ANGULAR CORRELATION FUNCTION

We wish to measure the two-point angular correlation function for both the full LCDCS catalog and for well-defined subsamples at $z\simeq0.45$ that we shall use to constrain the mass dependence of the correlation length. Gonzalez et al. (2001) find that the velocity dispersion is related to the peak surface brightness of the cluster detection via $\log\sigma \propto \log\Sigma(1+z)^{5.1}$, and so we employ this relation to define subsamples that are roughly velocity dispersion limited (see Figure 1). Error in the redshift dependence of this relation can induce a systematic bias in construction of our subsamples; however, this uncertainty is sufficiently small as to have negligible impact for the LCDCS data within the redshift range of the subsamples. We restrict all subsamples to $z>0.35$ to avoid sample incompleteness at lower redshift, while the maximum redshift (z=0.575) is set by sample size. Subsamples with larger redshift limits (and hence higher surface brightness limits) result in smaller samples ($N<100$) and correspondingly larger statistical uncertainties.

To compute the two-point angular correlation function, we use the estimator of Landy & Szalay (1993),

$$\omega(\theta) = \frac{n_r(n_r-1)}{n(n-1)}\frac{DD}{RR} - \frac{n_r-1}{n}\frac{DR}{RR} + 1, \qquad (1)$$

which Kerscher, Szapudi, & Szalay (2000) have demonstrated is more robust than other algorithms. In Equation 1, n is the number of clusters, n_r is the number of random points, DD is the number of cluster pairs with angular separation $\theta \pm \delta\theta/2$, RR is the number of random pairs with the same separation, and DR is the number of cluster-random pairs. To construct
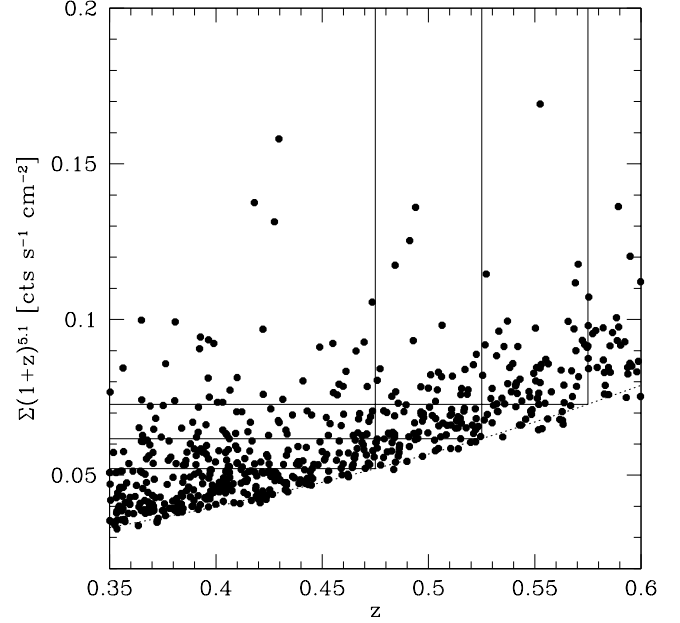

FIG. 1.— Extinction-corrected surface brightness distribution of the LCDCS clusters used to construct subsamples. The solid lines denote the redshift and $\Sigma(1+z)^{5.1}$ thresholds of the subsamples. The dotted curve is the surface brightness threshold of the full LCDCS catalog for E($B-V$)=0.05. Candidates at the detection threshold in lower extinction regions will lie slightly below this curve. Errors in the estimated redshifts move individual data points along tracks similar to this curve.

the random sample, we first generate a list of 44,000 random, unmasked locations within the survey region (2000 locations in each of the 22 scan sets that comprise the LCDCS survey). Next, we reject locations that fail any of the automated cluster selection criteria described in Gonzalez et al. (2001), yielding a final random sample of 33,886 positions.

Modelling the correlation function as a power law,

$$\omega(\theta) = A_\omega\theta^{1-\gamma} = \left(\frac{\theta}{\theta_0}\right)^{1-\gamma}, \qquad (2)$$

we use a maximum likelihood approach to determine the best-fit values for A_ω and γ. Similar to Croft et al. (1997) and Borgani, Plionis, & Kolokotronis (1999b), we maximize the likelihood function for an assumed Poisson probability distribution,

$$\mathcal{L} = \prod_i^N p_i = \prod_i^N \frac{\mu_i^{n_i}\exp(-\mu_i)}{n_i!}, \qquad (3)$$

where n_i and $\mu_i \equiv <DD>$ are the observed and expected number of pairs in the interval $d\theta$. The final results from the maximum likelihood analysis are not dependent upon the exact choice of $d\theta$, which can be made almost arbitrarily small. To determine the best-fit model parameters we use pairs with separations of $2' - 5^\circ$, and Monte Carlo simulations are utilized to determine the associated 1-σ uncertainties. Specifically, we use the best-fit parameters as initial values, generate 1000 random realizations of the cluster-cluster pair distribution, and then use the distribution of recovered parameter values to quantify the observational uncertainties. The angular correlation function for the entire LCDCS catalog and for our lowest redshift subsample are shown in Figure 2, overlaid with best-fit power law models. For the full LCDCS catalog, we obtain γ=-1.78 ± 0.10 and A_ω=-1.44 ± 0.04 (θ_0=51$\pm$22$''$).

z	$<z>$	N	$\log A_\omega$	γ	f	$\log A_{\omega,cor}$
(1)	(2)	(3)	(4)	(5)	(6)	(7)
All	0.56	1073	-1.44 ± 0.04	1.78 ± 0.10	0.29	-1.18 ± 0.04
0.35-0.475	0.42	178	-1.26 ± 0.17	2.15 ± 0.19	0.14	-1.13 ± 0.19
0.35-0.525	0.46	158	-1.35 ± 0.33	2.30 ± 0.33	0.16	-1.20 ± 0.33
0.35-0.575	0.50	115	-1.42 ± 0.47	2.51 ± 0.45	0.19	-1.24 ± 0.45
All	0.56	1073	-1.73 ± 0.05	2.15	0.29	-1.47 ± 0.05
0.35-0.475	0.42	178	-1.26 ± 0.13	2.15	0.14	-1.13 ± 0.13
0.35-0.525	0.46	158	-1.25 ± 0.14	2.15	0.16	-1.10 ± 0.14
0.35-0.575	0.50	115	-1.14 ± 0.18	2.15	0.19	-0.96 ± 0.18

Note — (1) Redshift range used to measure the angular correlation. (2) Number of clusters. (3) Values of $\log A_\omega$ are for θ in degrees. (7) Contamination-corrected amplitude of the angular correlation function. The second set of parameters in the table is for fixed values of the slope γ.

Table 1 lists information for the full LCDCS catalog and the three subsamples at $z\simeq0.45$, including the redshift range spanned by each subsample, the mean redshift of the subsample, the best-fit values of A_ω and γ, and the estimated fractional contamination. We also present best-fit values for A_ω fixing $\gamma=2.15$ — equivalent to the best-fit value for the lowest redshift subsample and similar to the best fit value for the ROSAT All-Sky Survey 1 Bright Sample (Moscardini et al. 2000, $\gamma=2.11^{+0.53}_{-0.56}$).

Because the LCDCS candidates are not spectroscopically confirmed, we must correct the correlation amplitude A_ω for the impact of contamination before this data can be used to derive the spatial correlation length r_0. If we assume that the contamination is spatially correlated and can be described by a power law with the same slope as the cluster angular correlation function (a reasonable approximation because for galaxies, which are likely the primary contaminant, $\gamma\simeq1.8$-1.9 (e.g. Roche & Eales 1999; Cabanac, de Lapparent, & Hickson 2000)), then the observed angular correlation function is

$$\omega(\theta) = A_\omega\theta^{1-\gamma} = \left(A_{\text{cluster}}(1-f)^2 + A_{\text{contamination}}f^2\right)\theta^{1-\gamma}, \quad (4)$$

where f is the fractional contamination. For detections induced by isolated galaxies of the same magnitude as BCG's at $z \simeq 0.35$ (and identified as galaxies by the automated identification criteria described in Gonzalez et al. 2001), we measure that A_{gal} is comparable to A_{ω_A}, the net clustering amplitude for all LCDCS candidates at $0.3<z<0.8$. For detections identified as low surface brightness galaxies (including some nearby dwarf galaxies) we measure $A_{\text{LSB}} \simeq 10A_{\omega_A}$. While these systems are strongly clustered, we expect that they comprise less than half of the contamination in the LCDCS. For multiple sources of contamination the effective clustering amplitude $A_{\text{contamination}} = \sum A_i f_i^2/(\sum f_i)^2$, so the effective clustering strength of the contamination is $A_{\text{contamination}} \lesssim 2.5A_{\omega_A}$ even including the LSB's.

The last column in Table 1 gives the contamination-corrected value of A_ω, under the assumption that $A_{\text{contamination}} = A_{\omega_A}$. If the effective correlation amplitude of the contamination is in the range $A_{\text{contamination}} = (0-2.5)A_{\omega_A}$ (which corresponds to uncorrelated contamination for the lower limit), then the systematic uncertainties in A_ω and the corresponding uncertainties in the

r_0 values derived in §5 are $\lesssim 1\%$. These uncertainties, which are small because the contamination only contributes to the observed correlation function with weight f^2, are far less than the statistical uncertainties in all cases. Uncertainty in the fractional contamination of the catalog yields a larger 6% systematic uncertainty in r_0, which is also less than the typical statistical uncertainty.

4. THE SPATIAL CORRELATION LENGTH

The observed angular correlation function can be used to determine the three-space correlation length if the redshift distribution of the sample is known. This is accomplished via the cosmological Limber inversion (Peebles 1980; Efstathiou et al. 1991; Hudon & Lilly 1996). For a power-law correlation function with redshift dependence $f(z)$,

$$\xi(r) = \left(\frac{r}{r_0}\right)^{-\gamma} \times f(z). \quad (5)$$

The corresponding comoving spatial correlation length is $r_0(z) = r_0 f(z)^{1/\gamma}$, and the Limber equation is

$$r_o^\gamma = A_\omega \frac{c}{H_0} \frac{\Gamma(\gamma/2)}{\Gamma(1/2)\Gamma[(\gamma-1)/2]} \times \quad (6)$$

$$\left[\frac{\int_{z1}^{z2}(dN/dz)^2 E(z)D_A(z)^{1-\gamma}f(z)(1+z)dz}{\left(\int_{z1}^{z2}(dN/dz)dz\right)^2}\right]^{-1}, \quad (7)$$

where dN/dz is the redshift distribution of objects in the sample, $D_A(z,\Omega_0,\Omega_\Lambda)$ is the angular diameter distance, and

$$E(z) = [\Omega(1+z)^3 + \Omega_R(1+z)^{-2} + \Omega_\Lambda]^{1/2}, \quad (8)$$

as defined in Peebles (1993). Because little evolution in the clustering is expected over the redshift intervals spanned by our subsamples (see the Appendix and Figure 3), $f(z)$ can safely be pulled out of the integral.

We estimate the true redshift distribution of clusters in each LCDCS subsample, dN/dz, based upon the observed distribution of estimated redshifts, dN_{obs}/dz. Because the redshift distribution of the full LCDCS catalog is slowly varying over the redshift interval probed by our subsamples, we are able to derive approximate models for the dN/dz of the subsamples by

TABLE 2
SPATIAL CORRELATION LENGTHS

z	ΛCDM ($\Omega_0 = 0.3$)		OCDM ($\Omega_0 = 0.3$)		τCDM(Γ=0.2)	
range	d_c	r_0	d_c	r_0	d_c	r_0
0.35-0.475	38.4	$14.7^{+2.0}_{-2.2}$	33.8	$12.9^{+1.7}_{-2.0}$	30.9	$11.8^{+1.5}_{-1.8}$
0.35-0.525	46.3	$16.2^{+2.7}_{-3.3}$	40.6	$14.2^{+2.3}_{-2.8}$	36.9	$12.9^{+2.1}_{-2.5}$
0.35-0.575	58.1	$18.2^{+4.0}_{-4.9}$	50.8	$15.8^{+3.4}_{-3.9}$	46.0	$14.4^{+3.1}_{-3.8}$

Note — The units for d_c and r_0 are h^{-1} Mpc. Listed uncertainties are statistical.
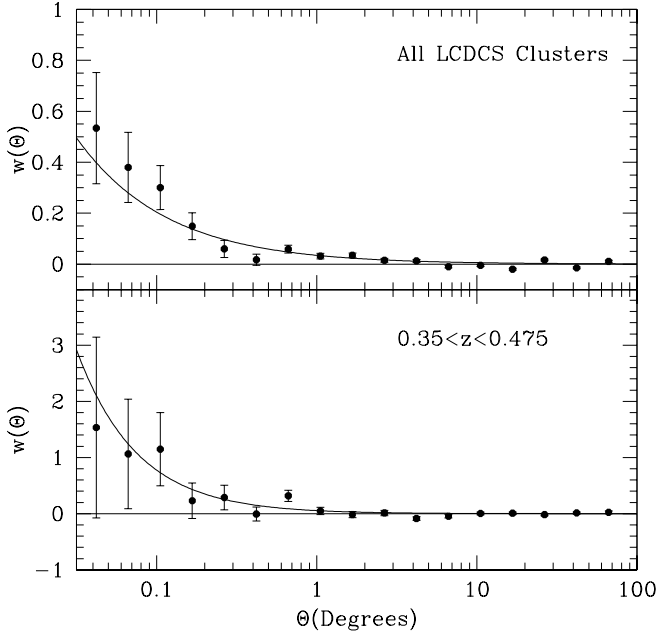
FIG. 2.— Angular correlation functions for the entire LCDCS catalog and for a volume-limited subsample with $0.35 \leq z < 0.475$. The solid lines are best-fit power law models, with the best-fit parameters given in Table 1. The data shown are plotted with bins of width $\Delta \log \theta$=0.2; for the actual maximum likelihood analysis of the subsamples we use $\Delta \log \theta$=0.005.

FIG. 3.— Comparison of the LCDCS data with local samples for a ΛCDM cosmology with Ω_0=0.3. The error bars on the LCDCS data correspond to the 1-σ statistical uncertainty. Overlaid are the results from the Virgo Consortium Hubble Volume simulations (Colberg et al. 2000) and analytic predictions (Γ=0.2) for z=0 and z=0.45. These fiducial curves do not account for the impact of uncertainty in cluster masses (see Figure 4).

convolving the dN_{obs}/dz with Gaussian scatter ($\sigma_z/z \approx 0.14$ at z=0.5; Gonzalez et al. 2001), which eliminates the sharp redshift limits imposed on z_{est} in construction of the subsamples. The rigorously correct method for obtaining the dN/dz is to *de*convolve the scatter; however, our approximation is sufficiently accurate for use in the Limber inversion because of both the slow variation of the LCDCS redshift distribution at this epoch and the weak dependence of the Limber inversion upon dN/dz. To test the validity of this approach, we also try modeling the dN/dz using the theoretical mass function of Sheth & Tormen (1999) convolved with redshift uncertainty. Comparing these two methods we find that the derived spatial correlation lengths agree to better than 3% for all subsamples. This result is insensitive to the exact mass threshold assumed for the theoretical mass function, again due to the weak dependence of the Limber inversion upon dN/dz.

5. RESULTS AND COMPARISON WITH LOCAL DATA

Table 2 lists the correlation lengths (r_0) and mean separations (d_c) that we derive for each of the three subsamples,
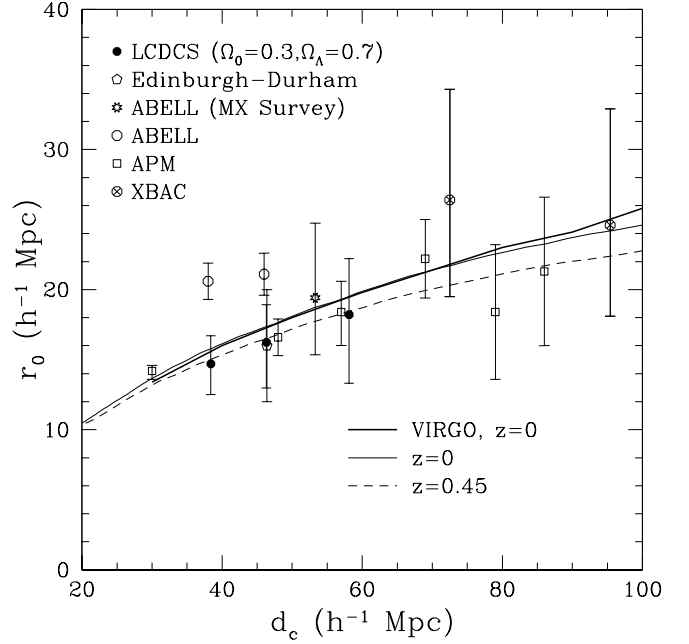
treating both γ and A_ω as free parameters. Both the r_0 and d_c values are cosmology-dependent, and so we list the derived values for ΛCDM (Ω_0=0.3), OCDM (Ω_0=0.3), and τCDM cosmologies. Values of d_c in Table 2 are computed as $d_c \equiv n^{-1/3} = [N(1-f)/V]^{-1/3}$, where N is the number of clusters, f is the contamination rate, and V is the effective comoving volume for a given subsample. Including the impact of Gaussian scatter upon the redshift distribution, the effective comoving volume for a subsample with redshift bounds z_1 and z_2 is

$$V = \delta\Omega \times \int_{z_1}^{z_2} dz\, p \frac{dV}{d\Omega dz} \qquad (9)$$

The effect of the redshift uncertainty is contained in p, which is the probability that a cluster at redshift z will be observed to have an estimated redshift within the redshift range spanned by the subsample. For Gaussian redshift scatter,

$$p(z) = \frac{\int_{z_1}^{z_2} dz'\, e^{-(z'-z)^2/2\sigma_z^2}}{\int_0^\infty dz'\, e^{-(z'-z)^2/2\sigma_z^2}}. \qquad (10)$$

Inclusion of p increases the computed values of d_c by $\sim$3%.

We compare the LCDCS results with several local studies to assess the degree of evolution between z=0.5 and the present epoch. We find that the LCDCS r_0 values are statistically consistent with results from the Edinburgh-Durham Galaxy Catalogue (Nichol et al. 1992), APM survey (Croft et al. 1997), and the MX Survey (northern sample, Miller et al. 1999), but smaller than the correlation lengths found by Peacock & West (1992) for their subsample of the Abell catalog. The correlation lengths from these studies are plotted in Figure 3, where the LCDCS data points are shown for an assumed ΛCDM cosmology (Ω_0=0.3). The lowest d_c data points for the XBAC catalog from Abadi, Lambas, & Muriel (1998), which probe higher masses than our study, are also plotted. We also include fiducial theoretical curves to illustrate the predicted degree of evolution between these epochs. The thick solid curve shows the z=0 results from the Virgo Consortium Hubble Volume simulations ($\Omega_0 = 0.3$, $\Omega_\Lambda = 0.7$, $\sigma_8 = 0.9$, Γ=0.17). The other two curves correspond to analytic predictions for the dependence of r_0 on d_c (or equivalently, on number density) at the two epochs, using the analytic model of Sheth & Tormen (1999) with Γ=0.2.

It is evident in Figure 3 that the weak evolution in the correlation length predicted for this ΛCDM model is consistent with the observations; however, for a more accurate comparison we should incorporate into the models the impact of observational scatter in the subsample mass thresholds for the different data sets. We restrict our attention to the APM and LCDCS catalogs in this analysis. For the APM catalog, we use the correlation lengths from Croft et al. (1997), taking the velocity dispersion scatter about the sample thresholds to be dlogσ=0.13 (based upon the data set of Alonso et al. 1999). We estimate the mean redshift of the APM samples to be $<z>\simeq$0.1. For the LCDCS catalog we use the surface brightness-velocity dispersion relation and surface brightness scatter from Gonzalez et al. (2001). The data and resulting models that include this scatter are shown in Figure 4a-c for the three cosmologies discussed in this paper. Both the APM and LCDCS data are consistent with the low-density models. For the plotted curves, the combined data sets yield reduced χ^2 values χ_ν^2=0.7 and χ_ν^2=0.6 for the ΛCDM and OCDM models, respectively.[3] In contrast, the plotted τCDM model systematically underpredicted the r_0 values for both data sets (χ^2=4.1 for Γ=0.2). τCDM can be made to better match the data by decreasing Γ; however, it is not possible to make τCDM simultaneously consistent with the cluster correlation length data and the galaxy power spectrum (e.g. Eisenstein & Zaldarriaga 2000).

6. SYSTEMATIC UNCERTAINTIES

It is important to consider whether any systematic biases have the potential to qualitatively alter our results. Table 3 summarizes the systematic effects discussed thus far in the text, as well as several additional potentially important factors. The most significant potential systematic bias is attributable to the impact of large scale structure. The LCDCS serendipitously includes the most X-ray luminous cluster known (RX J1347.5−1145 at z=0.45; Schindler et al. 1995). Three of the ten most massive LCDCS candidates with estimated redshifts $z_{est} \leq$0.58 have projected separations of less than 50 h^{-1} Mpc relative to RX J1347.5−1145, indicating that this region likely contains a massive supercluster. To estimate the sensitivity of our results to the presence of this region within the survey, we

recompute the correlation lengths excluding candidates within 100h^{-1} Mpc of RX J1347.5−1145. For all three subsamples the results change by less than 15% (i.e. less than $1-\sigma$), and for the lowest redshift subsample the correlation length actually increases slightly when this region is excluded. We thus conclude it likely that no individual supercluster should systematically alter our results by more that 15%.

Issue	Impact
	r_0
Large scale structure	$\lesssim$15%
Fractional contamination	6%
Clustering strength of contamination	$\lesssim$10%
Model for dN/dz in Limber equation	3%
Extinction-dependent selection effects	1%
Redshift dependence of Σ	<1%
Fixing γ. Would increase r_0 for subsamples (larger change for higher d_c bins)	0-10%
	d_c
Uncertainty in effective comoving volume	<3%

A second key concern, due to the cluster detection method, is whether there exist extinction-dependent selection effects that impact the derived correlation lengths. As a test we recompute r_0 for the lowest redshift subsample using only regions with E($B-V$)$\leq$0.06, which reduces the sample from 178 to 89 clusters. The recovered correlation length for these low-extinction regions is 13.2 (vs. 14.7 for all 178 clusters). This 10% change is less than the statistical uncertainty, indicating that our results are not strongly sensitive to variations in the galactic extinction within the survey region.

Of the factors previously discussed in the text, the greatest potential impact upon our results can be achieved if the *a priori* assumption is made that all subsamples have the same power law slope, γ. By making this assumption we test whether our results are robust to any factor that may be artificially enhancing the best-fit values of γ. If we fix γ=2.15, then the derived r_0 values for three subsamples increase by 0%, 6%, and 15% (in order of increasing maximum redshift for the subsamples). While these changes are less than the statistical uncertainties, they do act to steepen the slope of the observed r_0-d_c relation and thus slightly degrade the agreement with low-density models.

We next consider two additional issues that might qualitatively change the results of this paper. First, what if the redshift uncertainty is significantly larger than indicated by Gonzalez et al. (2001)? In this case the redshift ranges spanned by our subsamples are larger — and more similar to one another — than our current best assessment. If true, then we are currently underestimating r_0. Quantitatively, if σ_z/z=0.25 instead of 0.14, then the actual values of r_0 would be $\sim$2 h^{-1} Mpc larger. On the other hand, neither the mean separation d_c for a given sample or the steepness of the relation between r_0 and d_c changes perceptibly. Second, what if the contamination fraction is uniform in all the subsamples rather than being an increas-

---

[3] The bulk of the weight in computing these χ_ν^2 values comes from the APM data set. The LCDCS provides only slight additional leverage due to the large statistical uncertainties associated with these measurements.
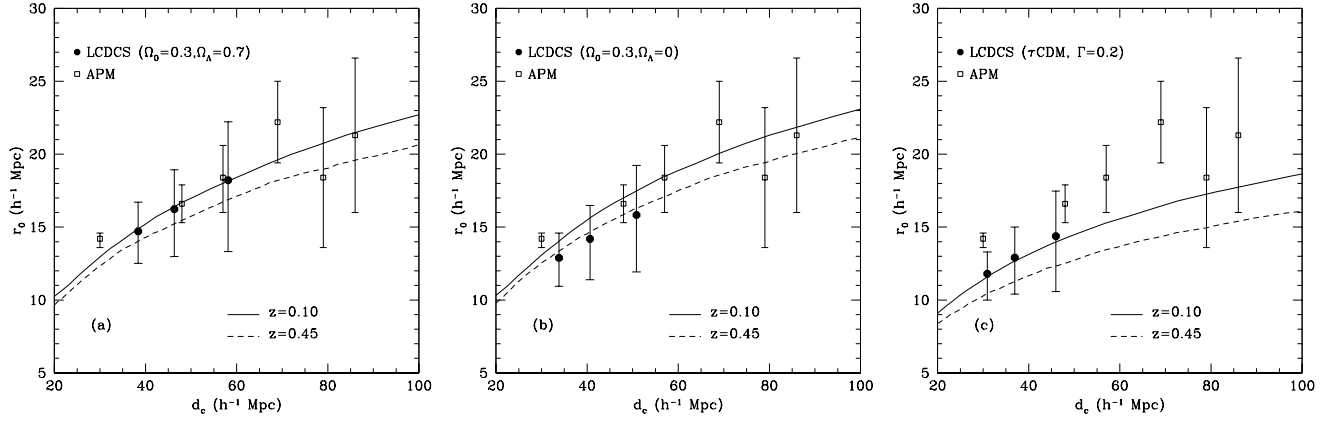
FIG. 4.— Comparison of the LCDCS and APM data sets with analytic predictions. Different panels correspond to the different cosmologies assumed in deriving the LCDCS correlation lengths (see Table 2). The analytic models include the impact of uncertainty in clusters masses for the two data sets, which causes these curves to be slightly shallower than the fiducial models in Figure 3.

ing function of redshift? Qualitatively, this would imply that part of the observed weak dependence of r_0 upon d_c is simply due to our contamination correction. Quantitatively, if we take the mean contamination rate to be 16% for all three subsamples, then the r_0 values(ΛCDM) change from (14.7,16.2,18.2) to (15.0,16.2,17.7) h^{-1} Mpc – a minor effect compared with other uncertainties.

From our analysis of the above systematics, we conclude that the two largest systematic uncertainties in this work arise from large scale structure and potential underestimation of the redshift uncertainty. Large scale structure can impact the derived values of r_0 at the $1-\sigma$, while underestimation of the redshift uncertainty could yield correlation lengths that are systematically too small (by up to ~ 2 h^{-1} Mpc if σ_z/z=0.25).

7. DISCUSSION AND CONCLUSIONS

The Las Campanas Distant Cluster Survey is the largest existing catalog of clusters at z>0.3, providing a unique sample with which to study the properties of the cluster population. We have used the LCDCS to constrain the cluster-cluster angular correlation function, providing the first measurements for a sample with a mean redshift $z\gtrsim$0.2. From the observed angular correlation function, we derive the spatial correlation length, r_0, as a function of mean separation, d_c. We find that the LCDCS correlation lengths are in agreement with results from local samples, and observe a dependence of r_0 upon d_c that is comparable to the results of Croft et al. (1997) for the APM catalog. This clustering strength, its dependence on number density, and its minimal redshift evolution are consistent with analytic expectations for low density models, and with results from the ΛCDM Hubble Volume simulations. Consequently, while statistical uncertainty limits our ability to discriminate between cosmological models, our results are in concordance with the flat ΛCDM model favored by recent supernovae and cosmic microwave background observations (e.g., Riess et al. 2001; Pryke et al. 2001; de Bernardis et al. 2001).

REFERENCES

Abadi, M. G., Lambas, D. G., & Muriel, H. 1998, ApJ, 507, 526
Alonso, M. V., Valotto, C., Lambas, D. G., & Muriel, H. 1999, MNRAS, 308, 618
Bahcall, N. A. 1988, ARA&A, 26, 631
Bahcall, N. A., & Soneira, R. M. 1983, ApJ, 270, 20
Bahcall, N. A., & West, M. J. 1992, ApJ, 392, 419
Baugh, C. M., Cole, S., & Frenk, C. S. 1998, ApJ, 498, 504
Borgani, S., Girardi, M., Yee, H. K. C., & Ellingson, E. 1999, ApJ, 527, 561
Borgani, S., Plionis, M., & Kolokotronis, V. 1999, MNRAS, 305, 866
Cabanac, R. A., de Lapparent, V., & Hickson, P. 2000, A&A, 364, 349
Colberg et al. 2000, MNRAS, 319, 209
Collins et al. 2000, MNRAS, 319, 939
Croft, R. A. C., Dalton, G. B., Efstathiou, G., Sutherland, W. J., & Maddox, S. J. 1997, MNRAS, 291, 305
Dalton, G. B., Croft, R. A. C., Efstathiou, G., Sutherland, W. J., Maddox, S. J., & Davis, M. 1994, MNRAS, 271, L47
Dalton, G. B., Efstathiou, G., Maddox, S. J., & Sutherland, W. J. 1992, ApJ, 390, L1
de Bernardis, P. et al. 2001, astro-ph/0105296
Dekel, A., Blumenthal, G. R., Primack, J. R., & Olivier, S. 1989, ApJ, 338, L5
Efstathiou, G., Bernstein, G., Katz, N., Tyson, A. J., & Guhathakurta, P. 1991, ApJ, 380, 47

Efstathiou, G., Dalton, G. B., Sutherland, W. J., Maddox, S. J., 1992, MNRAS, 257, 125
Eisenstein, D. J. & Zaldarriaga, M. 2000, ApJ, 546, 2001
Gonzalez, A. 2000, Ph.D. Thesis
Gonzalez, A. H., Zaritsky, D., Dalcanton, J. J., & Nelson, A. E. 2001, ApJS, ????
Governato, F., Babul, A., Quinn, T., Tozzi, P., Baugh, C. M., Katz, N., & Lake, G. 1999, MNRAS, 307, 949
Hudon, J. D., & Lilly, S. J. 1996, ApJ, 469, 519
Kerscher, M., Szapudi, I., & Szalay, A. S., ApJ, 535, 13
Kylpin, A. A., & Kopylov, A. I. 1983, Soviet Astronomy Letters, 9, 41
Landy, S. D., & Szalay, A. S. 1993, ApJ, 412, 64
Matarrese, S., Coles, P., Lucchin, F., & Moscardini, L. 1997, MNRAS, 286, 115
Miller, C. J., Batuski, D. J., Slinglend, K. A., Hill, J. M. 1999, ApJ, 523, 492
Mo, H. J., & White, S. D. M. 1996, MNRAS, 280, L19
Moscardini, L., Matarrese, S., De Grandi, S., & Lucchin, F. 2000, MNRAS, 314, 647
Nichol, R. C., Briel, O. G., Henry, P. J. 1994, ApJ, 267, 771
Nichol, R. C., Collins, C. A., Guzzo, L., Lumsden, S. L. 1992, MNRAS, 255, 21
Peacock, J. A. & West, M. J. 1992, MNRAS, 259, 494

Peebles, P. J. E. 1980, The Large-Scale Structure of the Universe (Princeton: Princeton University Press)

Peebles, P. J. E. 1993, Physical Cosmology (Princeton: Princeton University Press)

Postman, M., Huchra, J. P., & Geller, M. J. 1992, ApJ, 384, 404

Press, W. H. & Schechter, P. 1974, ApJ, 187, 425

Press, W. H., Teukolsky, S. A., Vetterling, W. T., Flannery, B. P. 1992, Numerical Recipes, (2nd ed.; New York: Cambridge University Press)

Pryke, C. et al. 2001, astro-ph/0104490

Roche, N., & Eales, S. A. 1999, MNRAS, 307, 703

Riess, A. G. et al. 2001, astro-ph/0104455

Romer, A. K., Collins, C. A., Böehringer, H., Cruddace, R. G., Ebeling, H., MacGillivray, H. T., Voges, W., 1994, Nature, 372, 75

Sadat, R., Blanchard, A., & Oukbir, J. 1998, A&A, 329, 21

Schindler, S., et al. 1995, A&A, 299, 9

Sheth, R. K., Mo, H. J., & Tormen, G. 2001, MNRAS, 323, 1

Sheth, R. K. & Tormen, G. 1999, MNRAS, 308, 119

Sutherland, W. 1988, MNRAS, 234, 159

van Haarlem, M. P., Frenk, C. S., & White, S. D. M. 1997, MNRAS, 287, 817

APPENDIX

ANALYTIC MODELS FOR THE SPATIAL CORRELATION FUNCTION

Analytic models for the spatial correlation function are based upon the Press-Schechter formalism (PS; Press & Schechter 1974) formalism. Mo & White (1996) were the first to use this formalism to derive the expected correlation for mass-dependent bias, finding that if the observed correlation function is defined as

$$\xi(r,z,M) = b^2(z,M)\xi_m(r,z),\tag{A1}$$

where ξ_m is the average mass correlation function,

$$\xi_m(r,z) = D_+^2(z)\int_0^\infty P(k)\frac{\sin kr}{kr}d^3k,\tag{A2}$$

then the bias, $b(z,M)$, is given by the equation

$$b(z,M) = 1 + \frac{\delta_c(z)}{\sigma^2(M)} - \frac{1}{\delta_c(z)}.\tag{A3}$$

Modeling of observed correlation functions requires calculation of the effective bias, $b_{eff}(z,M)$, which is the average of $b(z,M)$ weighted by the mass function of the clusters used to compute the correlation function (Mo & White 1996; Matarrese et al. 1997; Baugh, Cole, & Frenk 1998),

$$b_{eff} = \frac{\int_m^\infty b(M)n(M)dM}{\int_m^\infty n(M)dM},\tag{A4}$$

where m is the mass limit of the cluster sample.

This prescription can also be easily extended to incorporate the Sheth & Tormen modifications to PS by replacing equation (A3) with

$$b(z,M) = 1 + \frac{1}{\delta_c(0)}\left[\frac{a\delta_c^2(z)}{\sigma^2} - 1\right] + \frac{2p}{\delta_c(0)}\left[1 + \left(\frac{\sqrt{a}\delta_c}{\sigma}\right)^{2p}\right]^{-1}\tag{A5}$$

where a=0.707 and p=0.3 (Moscardini et al. 2000). This is the analytic model used in §5. For comparison, we also overlay results from the Virgo Consortium Hubble Volume simulations (Colberg et al. 2000) in Figure 3a.